

Constrained molecular dynamics simulation of the quark-gluon plasma

S. Terranova and A. Bonasera*

Laboratorio Nazionale del Sud, Istituto Nazionale Di Fisica Nucleare, Via S. Sofia 44, I-95123 Catania, Italy

(Received 22 December 2003; published 30 August 2004)

We calculate the equation of state of a quark system interacting through a phenomenological potential, the Richardson's potential, at finite baryon density and zero temperature. In particular we study three different cases with different quark masses (u and d), and different assumptions for the potential at large distances. We solve molecular dynamics with a constraint due to Pauli blocking and find evidence of a phase transition from "nuclear" to "quark matter." The phase transition is analyzed also through the behavior of the J/Ψ embedded in the quark system. We show that the J/Ψ particle behaves as an order parameter.

DOI: 10.1103/PhysRevC.70.024906

PACS number(s): 24.85.+p, 12.39.Pn, 21.65.+f

I. INTRODUCTION

The production of a state of matter, the quark-gluon plasma (QGP), is one of the open problems of modern physics. Theoretically, quantum chromodynamics (QCD) predicts such a state, QGP, but it can be applied only to some limited cases such as quark matter at zero density and high temperatures. Experimentally, such a system can be obtained through ultrarelativistic heavy ion collision (RHIC) at CERN and at Brookhaven [1]. QGP can be formed in the first stages of the collisions, and can be studied through the secondary particles produced. Some features of the quark matter can be revealed by studying the properties of hadrons in a dense medium. The particle J/Ψ is a good candidate because the formation of the QGP might lead to its suppression [2].

In this work we propose a semiclassical model which has an equation of state (EOS) resembling the well-known properties of nuclear matter and its transition to the QGP at zero temperature and finite baryon densities. We simulate the nuclear matter, which is composed of nucleons (which are by themselves composite three-quark objects), and its dissolution into quark matter. In addition, for our system of colored quarks, we will show how the color screening is related to the lifetime of the particle J/Ψ in the medium. In particular, we will see that the lifetime of the J/Ψ as a function of density behaves as an order parameter. Having a model which simulates the QGP might be useful when dealing with finite and, (possibly) out of equilibrium systems. In fact, dynamics and finite-size effects might wash out completely or hide a phase transition. The goal of our microscopic simulations is to help find unambiguous signals of the occurrence of the phase transition. In this work we will show that with using some phenomenological potential and suitably chosen quark masses we can indeed obtain an EOS which has some features of nuclear matter and its transition to the QGP. In fact, we stress that two systems having a similar EOS will behave the same. An important ingredient of our approach is a constraint to satisfy the Pauli principle. The approach, dubbed constrained molecular dynamics (CoMD) has been successfully applied to relativistic and nonrelativistic [3,4]

heavy-ion collisions and plasma physics as well [5].

The paper is organized as follows: in Sec. II we introduce the method, molecular dynamics with a constraint for fermions, CoMD. In Sec. III we apply the method to calculate the equation of state, with an arbitrary cutoff in the potential. In Sec. IV we use a screened linear potential and we calculate the EOS. In Sec. V there is a brief summary.

II. NUMERICAL METHOD

We use molecular dynamics with a constraint for a Fermi system of quarks with colors. The color degrees of freedom of quarks are taken into account through the Gell-Mann matrices and their dynamics are solved classically, in phase space, following the evolution of the distribution function. Starting from the quark degrees of freedom, some dynamical approaches have been proposed in Refs. [6–8] based on the Vlasov equation [9,10], and/or a molecular-dynamics-type approach. Of course, in such approaches it is important to get quark clusterization and the correct properties of nuclear matter (NM) at the ground-state (GS) baryon density $\rho_0 \sim 0.15 \text{ fm}^{-3}$ [11]. However, the property of ground-state nuclear matter, together with the high-density phenomena, is not sufficiently studied from the point of view of the quark degrees of freedom.

In our work, the quarks interact through the Richardson's potential $V(\mathbf{r}_i, \mathbf{r}_j)$,

$$V(\mathbf{r}_{i,j}) = 3 \sum_{a=1}^8 \frac{\lambda_i^a \lambda_j^a}{2 \cdot 2} \left[\frac{8\pi}{33 - 2n_f} \Lambda \left(\Lambda r_{ij} - \frac{f(\Lambda r_{ij})}{\Lambda r_{ij}} \right) \right], \quad (1)$$

and [12]

$$f(t) = 1 - 4 \int \frac{dq}{q} \frac{e^{-qt}}{[\ln(q^2 - 1)]^2 + \pi^2}. \quad (2)$$

λ^a are the Gell-Mann matrices. We fix the number of flavors $n_f=2$ and the parameter $\Lambda=0.25 \text{ GeV}$, ($\hbar, c=1$) unless otherwise stated. Here we assume the potential to be dependent on the relative coordinates only. The first term is the linear term, responsible for the confinement, the second term is the Coulomb term [13].

The exact (classical) one-body distribution function $f(\mathbf{r}, \mathbf{p}, t)$ satisfies the equation [10]

*Email address: terranova@lns.infn.it; bonasera@lns.infn.it

$$\partial_t f + \frac{\mathbf{p}}{E} \cdot \vec{\nabla}_{\mathbf{r}} f - \vec{\nabla}_{\mathbf{r}} U \cdot \vec{\nabla}_{\mathbf{p}} f = 0, \quad (3)$$

where $E = \sqrt{p^2 + m_q^2}$ is the energy, m_q is the (u, d) quark mass, and $U = U(\mathbf{r}) = \sum_j V(\mathbf{r}, \mathbf{r}_j)$. Numerically, Eq. (3) is solved by writing the one-body distribution function for each particle i through the delta function

$$f_i(\mathbf{r}, \mathbf{p}, t) = \sum_{\alpha=1}^Q \delta(\mathbf{r} - \mathbf{r}_\alpha) \delta(\mathbf{p} - \mathbf{p}_\alpha), \quad (4)$$

where $Q = q + \bar{q}$ is the total number of quarks (q) and anti-quarks (\bar{q}) (in this work $\bar{q} = 0$).

Inserting this expression in the exact equation (3) gives the Hamilton's equations

$$\frac{d\mathbf{r}_i}{dt} = \frac{\mathbf{p}_i}{E_i}, \quad (5)$$

$$\frac{d\mathbf{p}_i}{dt} = -\vec{\nabla}_{\mathbf{r}_i} U(\mathbf{r}). \quad (6)$$

Hence we must solve these equations of motion for our system of quarks.

Initially we distribute randomly the quarks in a box of side L in coordinate space and in a sphere of radius p_f in momentum space. p_f is the Fermi momentum estimated in a simple Fermi gas model by imposing that a cell in phase space of size $h = 2\pi$ can accommodate at most g_q identical quarks of different spins, flavors, and colors. $g_q = n_f \times n_c \times n_s$ is the degeneracy number, n_c is the number of colors (three different colors are used: red, green, and blue), hence $n_c = 3$, $n_s = 2$ is the number of spins [1].

A simple estimate gives the following relation between the density of quarks with colors, ρ_{qc} , and the Fermi momentum:

$$\rho_{qc} = \frac{3n_s}{6\pi^2} p_f^3. \quad (7)$$

We generate many events and take the average over all events in each cell on the phase space. For each particle we calculate the occupation average, i.e., the probability that a cell in the phase space is occupied. To describe the Fermionic nature of the system we impose that average occupation for each particle is less or equal to 1 ($\bar{f}_i \leq 1$).

At each time step we control the value of average distribution function, and consequently we change the momenta of particles by multiplying them by a quantity ξ : $P_i = P_i \times \xi$. ξ is greater or less than 1 if \bar{f}_i is greater or less than 1, respectively; which is the *constraint* [4].

With this procedure, the basic quantities describing the system, such as, total energy, average occupation, and order parameters, (they will be described in this section below), will reach stationary values after a given time. We can see this in Fig. 1 in a typical case with $\rho_B = 0.24 \text{ fm}^{-3}$. We have performed two calculations, under the same conditions, but with two different starting points, first from quarks with colors randomly distributed, i.e., QGP (left panels) and second

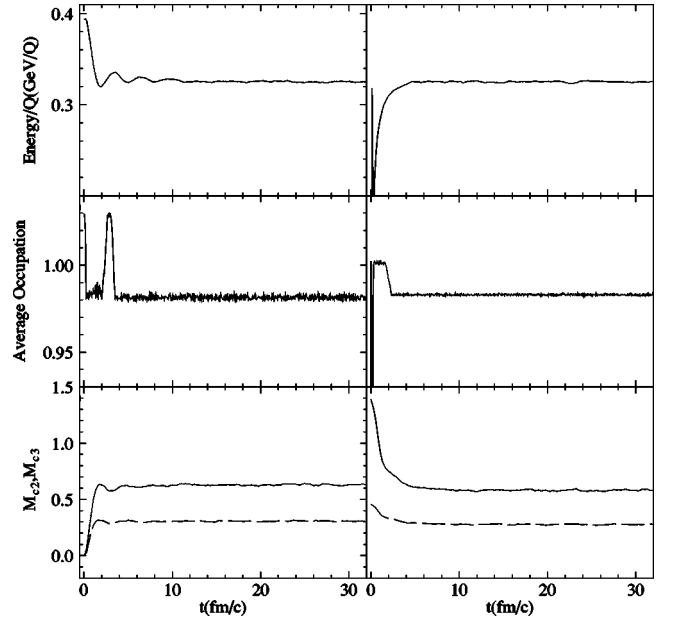


FIG. 1. Time evolution of energy per quark (top panel), average occupation (middle panel), and reduced order parameters (bottom panel), with different initial conditions: QGP (left panels) and nucleons (right panels).

from quarks condensed in clusters of three with different colors, i.e., nucleons (right panels), respectively. We can see that in both cases, the system reaches the same saturation value, though at different times. We stress that this behavior is independent of the density.

In the middle row of Fig. 1 we display the time dependence of the average occupation. It is greater than 1 when initially we distribute randomly the quarks in the box and later it approaches nearly 1 at saturation.

We define an order parameter to check the order of a phase transition, if any. It is defined through the Gell-Mann matrices as [3]

$$\begin{aligned} M_{c3} &= \frac{1}{N} \sum_{i=1}^N \sum_{a=3,8} \lambda_j^a \lambda_k^a + \lambda_i^a \lambda_j^a + \lambda_i^a \lambda_k^a \\ &= M_{c2} + \frac{1}{N} \sum_{a=3,8} \lambda_j^a \lambda_k^a + \lambda_i^a \lambda_k^a, \end{aligned} \quad (8)$$

where $j(i)$ and $k(i)$ are the two quarks closest to the quark i . M_{c2} is the reduced order parameter which gives the color of the particle j closest to a particular quark i .

In Fig. 1 (bottom) we show the time evolution of M_{c2} and M_{c3} when the quarks are initially randomly distributed in the system (left) and when they are clustered in nucleons (right), at the same conditions as above. The saturation values are equal in both cases, but the initial ones are different, 0 for the first case and close to $1/2$ and $3/2$, respectively, for M_{c2} and M_{c3} , for the second case. These values are typical for QGP and a system of nucleons, respectively, as we will show later in this section.

To better understand the clusterization of colored quarks we also define a higher-order parameter M_{c4} related to the colors of the four closest quarks

$$M_{c4} = \frac{1}{N} \sum_{i=1}^N \sum_{a=3,8} \lambda_j^a \lambda_k^a + \lambda_i^a \lambda_j^a + \lambda_j^a \lambda_l^a + \lambda_i^a \lambda_k^a + \lambda_k^a \lambda_l^a + \lambda_i^a \lambda_l^a, \quad (9)$$

where $l(i)$ is the third quark closest to the particular quark i .

We normalize the order parameters in this way

$$\tilde{M}_{c2} = \frac{2}{3}[M_{c2} + 1], \quad (10)$$

$$\tilde{M}_{c3} = \frac{2}{9}[M_{c3} + 3], \quad (11)$$

$$\tilde{M}_{c4} = \frac{2}{15}[M_{c4} + 6]. \quad (12)$$

From the properties of the Gell-Mann matrices [14] it is easy to derive the following results for the order parameters: if the three closest quarks have different colors, then $\tilde{M}_{c2} = 1$ ($M_{c2}=1/2$), $\tilde{M}_{c3}=1$ ($M_{c3}=3/2$), and $\tilde{M}_{c4}=1$ ($M_{c4}=3/2$). In fact the fourth quark will have the same color of one of the first three; in this case we have isolated white nucleons. This case is recovered in the calculation at small densities, where the system is locally invariant for rotation in color space.

If the four closest quarks have the same color $\tilde{M}_{c2}=\tilde{M}_{c3}=\tilde{M}_{c4}=0$, we have a condition that we call exotic color clustering. Also in this case the system is locally invariant for rotation in color space. The corresponding potential energy is very large and repulsive.

If the three closest quarks have two different colors, independently of the color of the two closest quarks, i.e., the color of the closest particle to quark i is randomly chosen, we have the quark-gluon plasma, hence: $\tilde{M}_{c2}=\tilde{M}_{c3}=\frac{2}{3}$. In this state \tilde{M}_{c4} can assume three different values: $\frac{4}{5}$; 1; $\frac{3}{5}$, according to the colors of the four closest quarks and number of pairs of different color. If we have two pair of quarks with the same color (e.g., $rggr$) $\tilde{M}_{c4}=\frac{4}{5}$. If the quarks have three different colors and two of the first three have two different colors (e.g., $rggb$) $\tilde{M}_{c4}=1$. If instead three of the four closest quarks have the same color, but the first three have two different colors (e.g., $rggg$), $\tilde{M}_{c4}=\frac{3}{5}$. In the next sections we will analyze these quantities better in different conditions. We note that in the QGP case the system is globally invariant for rotation in color space.

To test for a signature of the various states of matter we studied the behavior of a pair of quarks c and \bar{c} embedded in the system, with $m_c=m_{\bar{c}}=1.37$ GeV. For each density we calculate the lifetime of the J/Ψ particle, through its survival probability in the system. The J/Ψ embedded in matter might breakup, essentially for two reasons. The first is that the internal kinetic energy of the (c, \bar{c}) pair is large compared to the mutual attraction of the components (this is true in the

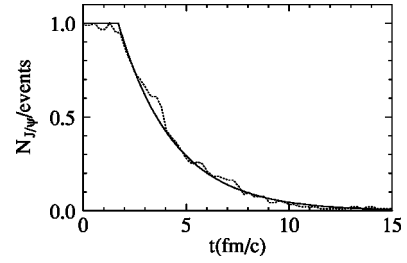


FIG. 2. Time evolution of surviving J/Ψ 's.

case where the interaction is neglected—which we will discuss below). The second, and most important reason, is that other quarks interact with the bound pair, eventually splitting it. Intuitively, it is clear that the splitting occurs faster at higher densities where the (c, \bar{c}) pair interacts with many other lighter quarks. The survival probability is related to the total number of pairs c and \bar{c} that stay bound after they are inserted in our saturated system of u and d quarks. We have made a fit to the J/ψ survival probability with the expression

$$P_{sur}(t) = \exp[-(t - t_D)/\tau] \quad (13)$$

and

$$t_{sur} = t_D + \tau, \quad (14)$$

where t_D is the delay time of the J/ψ before the probability exponentially decreases, and t_{sur} is the lifetime of J/ψ in the system, similar to fission [15]. A typical example of the fit is given in Fig. 2, where the dotted line is an example of the real distribution and the full line is obtained through Eq. (13).

In our study of the equation of state of quark matter at various baryon densities we look for some evidence of a phase transition to QGP also through the properties of the meson J/Ψ in the medium. This is important because we want to see if the J/Ψ can tell us about the occurrence and the order of the phase transitions. In future works for finite systems we want to test if the properties of the J/Ψ remain. In fact, in an infinite system there is unlimited time for dissolving the J/Ψ , but in a rapidly expanding QGP this dissolution might not occur, also because of the relatively large charm mass.

III. RESULTS WITH CUTOFF

When quarks, objects of different colors, are embedded in a dense medium such as in nuclear matter, the potential becomes screened in a similar fashion to ions and electrons in condensed matter. This is the *Debye screening* [1,10]. The screening can be obtained through the use of a Debye radius in the interaction, as will be discussed in the next section. In this section, the screening is produced directly, through the interaction of colored quarks. But our system is not really an infinite system, like nuclear matter, and this screening is insufficient to screen the linear potential and avoid its divergence for $r \rightarrow \infty$, hence we introduce a cutoff for the potential. The cut-off is a free parameter. When quark distances are greater than the cutoff, the interaction is equal to zero. Of

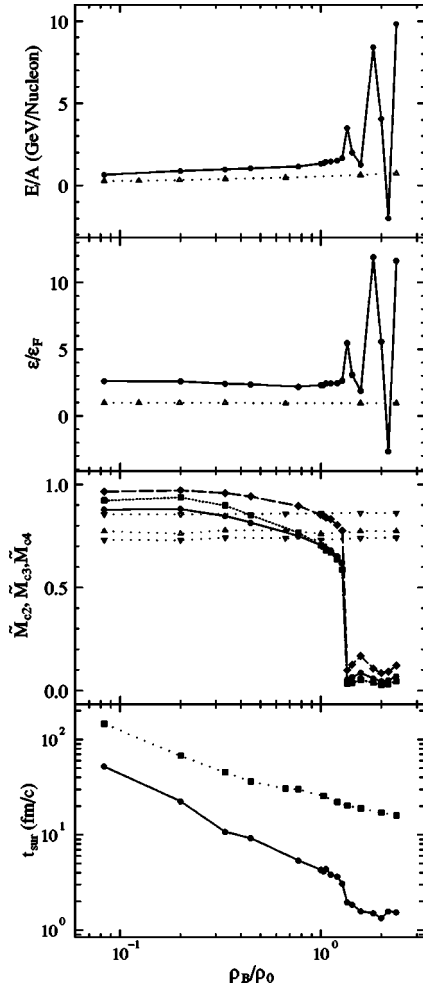


FIG. 3. Energy per nucleon (top panel), energy density (second to top), normalized order parameters (third panel), and time survival of J/ψ (bottom panel) vs density divided by the normal density ρ_0 , for $m_u=5$ MeV, $m_d=10$ MeV, and cutoff=3 fm.

course, we are aware that by using a cutoff in the linear term, the confinement property of the quarks might be lost. Nevertheless we will show that this prescription leads to interesting effects which might be used in finite system studies. Furthermore, the cutoff is relatively large, thus it takes considerable energy to have isolated quarks.

In Fig. 3 we plot some quantities related to the case with small quark masses, $m_u=5$ MeV, $m_d=10$ MeV, and a cutoff of 3 fm.

The energy per nucleon and the corresponding energy density in units of ϵ_F (energy density for a Fermi gas [1]) (top panels) versus baryon density divided by the normal density ρ_0 , have a very irregular behavior that we can explain through the order parameters (third panel).

For small densities the quarks are condensed in clusters of three different colors, the system is locally white (isolated white nucleon). The normalized order parameters \tilde{M}_{c_2} (circles), \tilde{M}_{c_3} (squares), and \tilde{M}_{c_4} (diamonds) are near to 1, hence the two closest particles to quark i have different colors and consequently the third closest quark to i has the same color of one of the first two or of i , $\tilde{M}_{c_2}=\tilde{M}_{c_3}=\tilde{M}_{c_4}\approx 1$. At

higher densities, the quarks are not in clusters but randomly distributed, $\tilde{M}_{c_2}=\tilde{M}_{c_3}\approx\frac{2}{3}$ and $\tilde{M}_{c_4}\approx\frac{4}{5}$, and we have the QGP ($\rho_B/\rho_0\sim 1.2$). But the system does not stay in this state, it prefers the exotic color clustering state, where at least the four closest quarks have the same color. At a density of about 1.4–2.4 times the normal density, $\tilde{M}_{c_2}=\tilde{M}_{c_3}=\tilde{M}_{c_4}\approx 0$. The system reaches this state through a first-order phase transition [1] at about 1.3 times the normal nuclear matter density. In the figure pertaining to the energy per nucleon, the transition is signaled by a discontinuity at the same density. The other discontinuities at larger densities ($\rho_B/\rho_0>1.5$), are probably due to the clusterization of more than four quarks of the same color. The reason for the phase transition at such a small density is because of the small quark masses and the large cut-off radius. As we will show more in detail below, we can change those values and change not only the density where the transition occurs, but also the order of the transition, if any.

In the present conditions, the linear term becomes very large and positive, hence the attraction between different clusters of quarks with different colors, far apart in space, prevails over the repulsion between charges of the same color in each cluster; this explains the large values of the energy and consequently of energy density. For instance, we might have the formation of a three-red-quark cluster and this is attracted by an analogous three-green-quark cluster.

It is the linear term that produces this very irregular behavior. In fact, repeating the same calculations with the Coulomb term only (triangles in Fig. 3), we obtain a constant contribution, not only to the energy, but also to the order parameters. The Coulomb term produces a permanent clusterization among quarks, which prevents them from reaching the ideal QGP state. In fact, the density dependence of the Coulomb term is similar to the Fermi energy term. The difference between the two terms depends on the α_s value, where α_s is the strong constant coupling defined in the potential through the Λ parameter. When the linear term is included it prevails with respect to the Coulomb one and the system stays in an exotic color clustering state, $\tilde{M}_{c_2}=\tilde{M}_{c_3}=\tilde{M}_{c_4}=0$.

In Fig. 3 (bottom) we plot the lifetime of J/Ψ versus baryon density divided by ρ_0 (full line). When the density increases, the lifetime decreases because it is more probable that a particle of different flavor gets in between a $c\bar{c}$ pair and breaks the bond, thus the number of surviving J/Ψ 's in the medium decreases faster and we have small values of t_{sur} .

t_{sur} behaves similarly to an order parameter; in fact, it has a jump just where we found the phase transition ($\rho_B/\rho_0\sim 1.3$). Analyzing the particle J/Ψ in the medium, by turning off the interaction (squares in the bottom of Fig. 3), gives a different behavior, viz., a monotonic decrease with density. The survival time in the medium is always larger than that with interaction, because the forces break more easily the bonds between particles (c,\bar{c} quarks). After the jump we notice a saturation of the surviving probability, again similar to the order parameter. We would like to note that even though there is not much similarity between the EOS obtained here and nuclear matter with its transition to the QGP, it was the first case we studied and its features are quite general, as we

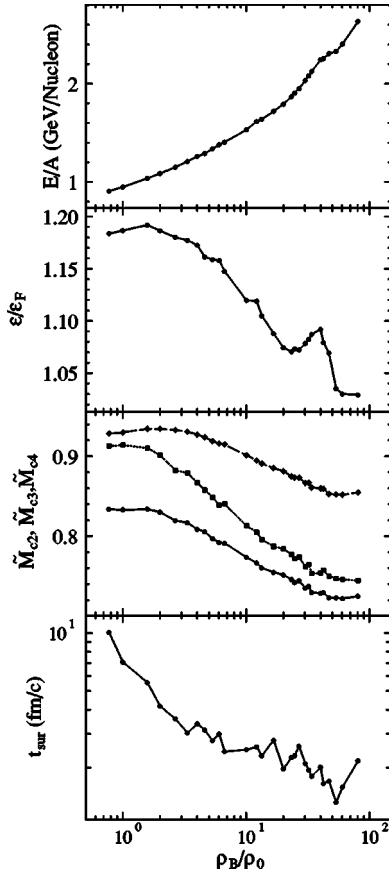


FIG. 4. Energy per nucleon (top panel), energy density (second to top panel), normalized order parameters (third panel), and time survival of J/ψ (bottom panel) versus density divided by the normal density ρ_0 for $m_u=m_d=180$ MeV, and a cutoff of 1.26 fm.

will see in the following. In fact, a simple scaling around the critical density would suffice to compare to the other systems. We notice also that even though the J/ψ is usually studied at zero density and finite temperatures, we expect a similar behavior to the one discussed here, with the Fermi motion playing the role of the temperature.

In order to study the sensitivity of the results to the input parameters, we have repeated the calculations with $m_u=180$ MeV, $m_d=180$ MeV, and a cutoff equal to 1.26 fm. The quark masses are chosen to reproduce the energy per nucleon of nuclear matter at normal density [11]. In Fig. 4 where we plot the same quantities of Fig. 3 (the symbols have the same meaning), we can see a behavior more regular than we did previously. At very high densities (almost 45 times the normal density), in the figure relative to the energy per nucleon (top) we see a flex, probably indicating a second-order phase transition, which becomes a change of slope in energy density (figure below). The normalized order parameters are always positive, i.e., it never happens that three equal quark color states are, on average, in the same region in r space. At low densities actually they never reach the value of 1 (nucleons), which implies that our potential is insufficient to get a good clusterization. In fact, we do not obtain the minimum in energy per nucleon, indicating a condition of stability for the system.

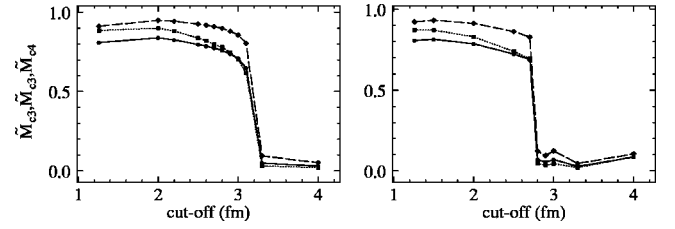


FIG. 5. Reduced order parameters vs cutoff for $m_u=5$ MeV, $m_d=10$ at two different densities.

Values of order parameters at high density are always larger than $2/3$ for \tilde{M}_{c2} and \tilde{M}_{c3} , and $4/5$ for \tilde{M}_{c4} (one of the possible values of \tilde{M}_{c4} to have QGP). This indicates a residual clusterization between quarks of different color, which we associate to the semiclassical counterpart of pairing. In fact, a residual attractive force, especially due to the Coulomb term, couples quarks of different color.

Also in this case we studied the behavior of the J/ψ in the medium and we obtained a regular behavior for the lifetime, see Fig. 4 (bottom), i.e., a fast decrease for small densities and after about $7\rho_0$ a slow decrease with some fluctuation around $1\sim 2$ fm/c. The lifetime of J/ψ again behaves similarly to the order parameters. In conclusion, we can see that changing quark masses and cutoffs does not result in exotic color clustering and a first-order phase transition, but a probable second-order phase transition to QGP.

It is clear that the cut-off value affects the transition point as a consequence. In Fig. 5 we plot the reduced order parameters \tilde{M}_{c2} , \tilde{M}_{c3} , \tilde{M}_{c4} versus cutoff at a density $\rho_B=\rho_0$ (left) and at $\rho_B=0.3558$ fm $^{-3}$ ($\sim 2.3\rho_0$) (right) for $m_u=5$ MeV, $m_d=10$ MeV. Changing the cut-off value from 1.26 to 4 fm results in a phase transition changing from QGP to an exotic color clustering state, at 3.1 fm for smaller density and at 2.7 fm for $\rho_B=0.3558$ fm $^{-3}$, while the system was in a nucleonic state for small cut-off values for both cases.

At $\rho_B=3.49$ fm $^{-3}$ ($\sim 23.26\rho_0$) we calculated the order parameters versus cutoff, shown in Fig. 6, for $m_u=m_d=180$ MeV (left) and versus quark masses for a cutoff = 1.26 fm (right). As in the previous case with smaller quark masses, Fig. 5, for small cut-off values we have typical values of a nucleonic state. When the cutoff increases we have a phase transition from QGP to an exotic color clustering state, at a cutoff equal to 2.3 fm. If we analyze the reduced order parameters versus quark masses we find an almost constant behavior. Very large variations of quark masses correspond to small variations of the \tilde{M}_{c2} , \tilde{M}_{c3} , \tilde{M}_{c4} values, hence the

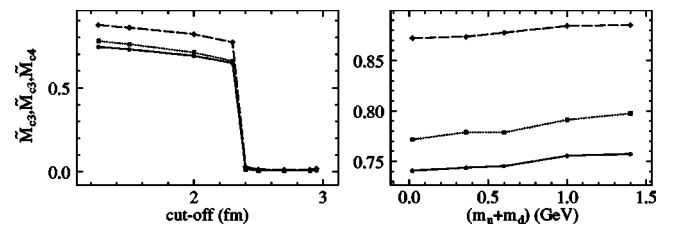


FIG. 6. Reduced order parameters vs cutoff for $m_u=m_d=0.18$ MeV and vs quark masses for cutoff=1.26 fm.

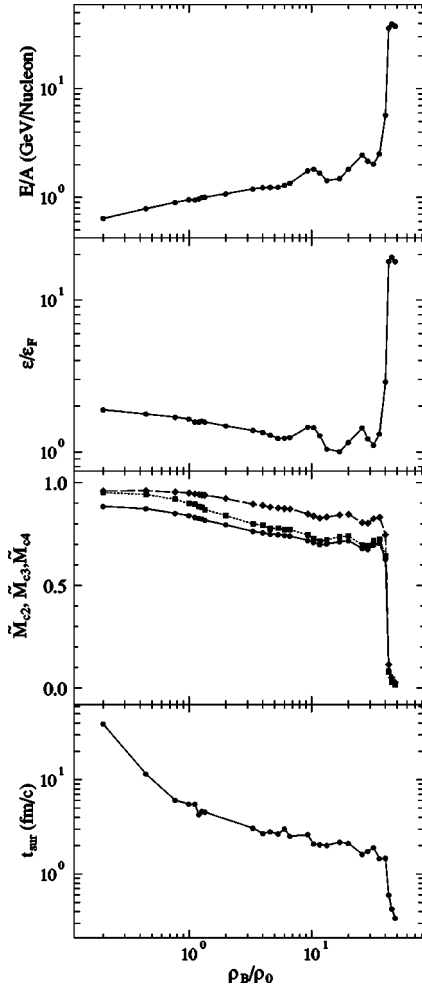


FIG. 7. Energy per nucleon (top panel), energy density (second to top panel), normalized order parameters (third panel), and time survival of J/ψ (bottom panel) versus density divided by the normal density ρ_0 for $m_u=5$ MeV, $m_d=10$ MeV and cutoff=2 fm.

cutoff is mainly responsible for the phase transition at different densities.

This suggests the use of a different cut-off value to change the point of transition. In Fig. 7, we plot the energy per nucleon, the energy density, the normalized order parameters, and the time survival of J/ψ , for $m_u=5$ MeV, $m_d=10$ MeV, and cutoff=2 fm.

At $\rho_B=\rho_0$ the total energy per nucleon (top) has a value similar to the typical value of nuclear matter, but we do not have the expected minimum. Important physics is in fact missing in our approach to describe the system of quark at small densities, i.e., the nuclear part. At $\rho_B=10\rho_0$ the energy per nucleon and energy density (second to top) displays some fluctuations near the QGP state. In fact, the value of the reduced order parameters (third panel) are close to 2/3 for \tilde{M}_{c2} , \tilde{M}_{c3} and 4/5 for \tilde{M}_{c4} . Increasing the density further gives a first-order phase transition to exotic color clustering state at $\rho_B \sim 40\rho_0$, as signaled by the reduced order parameters $\tilde{M}_{c2}=\tilde{M}_{c3}=\tilde{M}_{c4} \approx 0$ and the large increase of energy and energy density. The lifetime of the J/Ψ particle displays some fluctuations around $10\rho_0$ and a jump around $40\rho_0$, simi-

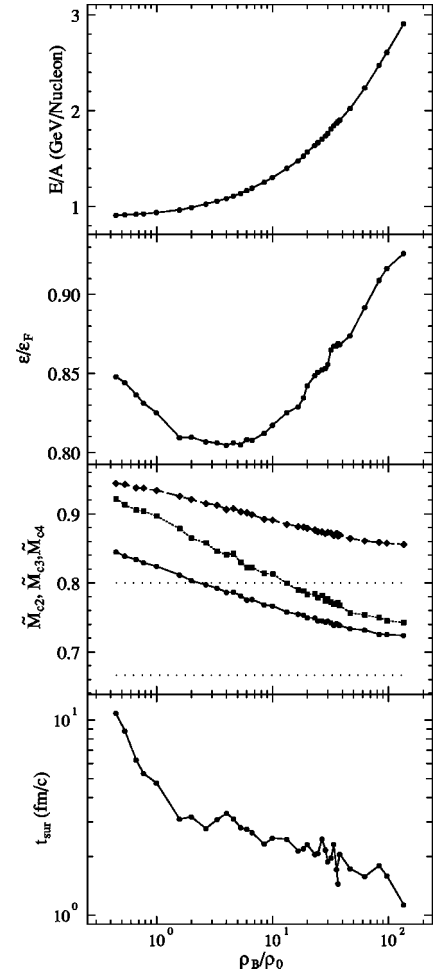


FIG. 8. Energy per nucleon (top panel), energy density (second to top panel), normalized order parameters (third panel), and time survival of J/ψ (bottom panel) versus density divided by the normal density ρ_0 for $m_u=m_d=324$ MeV.

lar to the behavior of the reduced order parameters. This equation of state could be our initial condition to simulate a finite system and a collision between nuclei.

IV. DEBYE SCREENING

In this section, to have a good screening of the linear interaction we use a particular expression of the linear term obtained through the resolution of the Poisson equation in one dimension [16]

$$\nabla^2 \phi_{Lin} = - \sum_i q_i \rho_{qi}, \quad (15)$$

where ρ_{qi} is the linear density obtained in the Thomas-Fermi approximation

$$\rho_{qi} \approx \frac{E_{F_0}}{(6\pi^2)^{1/3}} \left[\left(1 - \frac{\phi_{Lin}}{E_{F_0}} \right)^2 - \frac{m_q^2}{E_{F_0}^2} \right]^{1/2}. \quad (16)$$

E_{F_0} is the Fermi energy calculated at large distances, where the field $\phi_{Lin}(r) \rightarrow 0$ and $P_{F_0} = (6\pi^2/g_q \rho_{q0})^{1/3}$, i.e., we

require that all the r dependence is contained in the field and the density reduces to the free one for large distances from a given quark. Hence,

$$\phi_{lin} = \begin{cases} \frac{K}{\chi_l} \exp(-\chi_l r_{ij}) & \rho_q \neq 0 \\ Kr_{ij} & \rho_q = 0 \end{cases},$$

with

$$\chi_l^2 = \frac{4}{\sqrt{3}} K \left(\frac{g_q}{6\pi^2} \right)^{1/3} \frac{\sqrt{P_F^2 + m_q^2}}{P_F}. \quad (17)$$

χ_l is the linear Debye inverse radius [16], which for large densities go to a constant. Also the linear potential goes to a constant and not to zero like for a total screening, but for distance larger than the Debye radius, the potential is screened. K is the string tension defined through the Λ parameter [14]. We stress that the confinement property is recovered in the zero density limit.

In Fig. 8 we plot some results with this potential and $m_u = m_d = 324$ MeV. Again in this case we choose the masses of quarks to reproduce the energy per nucleon of nuclear matter at normal density.

In the top panel of Fig. 8, relative to energy per nucleon we find a minimum for low densities. The energy density, for large densities, shows some fluctuations, which may be due to numerical fluctuations.

The order parameters are smooth functions of the density and also in this case they never reach the QGP values (dotted line): $\tilde{M}_{c2} = \tilde{M}_{c3} = \frac{2}{3}$ and $\tilde{M}_{c4} = \frac{4}{5}$ (or other possible values), i.e., a residual clusterization remains. Probably it is an effect of the instability of quark pairs of different colors that produces the instability at large energy densities. Also, in this case the reduced order parameters are always positive, and we never have exotic color clustering. The calculated lifetime of J/Ψ in the medium versus density is shown in Fig. 8 (bottom) and it behaves like the order parameters.

V. SUMMARY

In conclusion, in this work we have discussed a semiclassical molecular dynamics approach to infinite matter at finite baryon densities and zero temperature starting from a phenomenological potential that describes the interaction between quarks with color. Pauli blocking, necessary for fermions at zero temperature, is enforced through a constraint to the average one-body occupation function. Color degrees of freedom for quarks are responsible for Debye screening, even though we have adopted some prescription mainly for numerical reasons to screen the linear term at large distances. Depending on parameters for the quark masses and the potential, we obtain an EOS which exhibits a first, second, or a simple crossover to the QGP. We stress that these transitions are due to changes in the system symmetries. In fact, we have a local invariance for rotation at low densities, i.e., for nucleons. This means that we can rotate locally the color of the quarks with no change in the energy. The QGP displays a global invariance, i.e., we can change randomly the quarks colors anywhere in the system without changing the system properties. Exotic color clustering is also a local property, in fact, we can change the color randomly, but only within a cluster of identical colors. It is the breaking of these symmetries that gives the phase transitions. A suitable physical observable for the phase transition could be the J/Ψ . In fact, we have shown that for infinite systems it behaves like an order parameter and it is also able to distinguish between a first-order and a second-order (or a crossover) phase transition. Finite-size and dynamical studies within the model proposed will reveal if such a property remains. Those studies could also give indications on the possibility that the phase transitions are washed out by finite-size effects. Also, other indicators of a phase transition such as intermittency can be easily studied in the framework of our model.

ACKNOWLEDGMENT

We thank J. Winfield for carefully reading the manuscript.

-
- [1] C. Y. Wong, *Introduction to High-Energy Heavy Ion Collisions* (World Scientific, Singapore, 1994); L. P. Csernai, *Introduction to Relativistic Heavy Ion Collisions* (Wiley, New York, 1994).
 - [2] R. C. Hwa, *Quark-Gluon Plasma* (World Scientific, Singapore, 1990).
 - [3] A. Bonasera, Phys. Rev. C **62**, 052202(R) (2000).
 - [4] M. Papa, T. Maruyama, A. Bonasera, Phys. Rev. C **64**, 024612 (2001).
 - [5] A. Bonasera, Prog. Theor. Phys. Suppl. **154**, 261 (2004).
 - [6] A. Bonasera, Phys. Rev. C **60**, 65212 (1999); Nucl. Phys. **A681**, 64c (2001).
 - [7] T. Maruyama and T. Hatsuda, Phys. Rev. C **61**, 62201(R) (2000).
 - [8] T. Vetter, T. Biro, and U. Mosel, Nucl. Phys. **A581**, 598 (1995); S. Loh, T. Biro, U. Mosel, and M. Thoma, Phys. Lett. B **387**, 685 (1996); S. Loh, C. Greiner, U. Mosel, and M. Thoma, Nucl. Phys. **A619**, 321 (1997); S. Loh, C. Greiner, and U. Mosel, Phys. Lett. B **404**, 238 (1997), and references therein.
 - [9] A. Bonasera, F. Gulminelli, and J. Molitoris, Phys. Rep. **243**, 1 (1994); G. Bertsch and S. Dasgupta, *ibid.* **160**, 189 (1988), and references therein.
 - [10] E. M. Lifshitz and L. P. Pitaevskii, *Physical Kinetics* (Pergamon, New York, 1991).
 - [11] B. Povh, K. Rith, C. Scholz, and F. Zetsche, *Particles and Nuclei: An Introduction to the Physical Concepts* (Springer, Berlin, 1995).
 - [12] J. L. Richardson, Phys. Lett. **82B**, 272 (1979).

- [13] A. Bonasera, nucl-th/9905025; Phys. Rev. C **60** 065212 (1999).
- [14] R. Morpurgo, *Introduzione alla Fisica delle Particelle* (Zanichelli, Bologna, Italy, 1987).
- [15] T. Maruyama, A. Bonasera, M. Papa, and S. Chiba, Eur. Phys. J. A **14**, 191 (2002).
- [16] L. Landau and E. Lifshitz, *Statistical Physical* (Pergamon, New York, 1980).